Published May 1, 1972

THE CILIARY NECKLACE

A Ciliary Membrane Specialization

NORTON B. GILULA and PETER SATIR

From the Department of Physiology-Anatomy, University of California, Berkeley, California 94720. Dr. Gilula's present address is the Department of Anatomy, Harvard Medical School, Boston, Massachusetts 02115.

ABSTRACT

Cilia, primarily of the lamellibranch gill (*Elliptio* and *Mytilus*), have been examined in freeze-etch replicas. Without etching, cross fractures rarely reveal the 9 + 2 pattern, although suggestions of ninefold symmetry are present. In etched preparations, longitudinal fractures through the matrix show a triplet spoke alignment corresponding to the spoke periodicity seen in thin sections. Dynein rows can be visualized along the peripheral microtubules in some preparations. Fracture faces of the ciliary membrane are smooth with few membrane particles, except in the regions adjacent to the basal plate. In the transition region below the plate, a unique particle arrangement, the ciliary necklace, is found. In the *Elliptio* gill, on fracture face A the necklace is comprised of three well-defined rows or strands of membrane particles that encircle the ciliary shaft. The rows are scalloped and each scallop corresponds to a peripheral doublet microtubule. In thin sections at the level of these particles, a series of champagne-glass structures link the microtubular doublets to the ciliary membrane. The ciliary necklace and this "membrane-microtubule" complex may be involved in energy transduction or the timing of ciliary beat. Comparative studies show that these features are present in all somatic cilia examined including those of the ameboflagellate *Tetramitus*, sea urchin embryos, rat trachea, and nonmotile cilia of cultured chick embryo fibroblasts. The number of necklace strands differs with each species. The necklace has not been found in rat or sea urchin sperm.

INTRODUCTION

General features of eukaryotic cilia and flagella, in particular their 9 + 2 microtubular arrangement, have been extensively studied since the advent of biological electron microscopy (Manton and Clark, 1952; Fawcett and Porter, 1954; Afzelius, 1959; Gibbons and Grimstone, 1960; Satir, 1965). The cilium is an internal organelle, completely enclosed by what at first appears to be a simple extension of the cell membrane (Porter, 1957). In thin section, the ciliary membrane is a typical "unit membrane." However, there are certain indications of cytochemical and possibly physiological differences between the ciliary membrane and other portions of the cell membrane. For example, we have recently shown that the ciliary membrane does not precipitate pyroantimonate to the same extent as the adjacent cell and microvillar membranes (Satir and Gilula, 1970 a). This may mean that the ion-binding properties of the ciliary and adjacent membranes differ. Again, although the ciliary membrane seems to be osmotically active (Satir and Jacobson, unpublished

results), its permeability properties may well be unique (Ronkin and Buretz, 1960; Steinbach and Dunham, 1962).

Isolated ciliary membranes can be obtained for biochemical analysis (Gibbons, 1963, 1967). The membrane is soluble in detergents such as digitonin. About 22% of the total protein, or 31% of the nonmatrix protein, of the cilium is present in the isolated membrane fraction. The membrane contains a Mg^{++}-activated adenosine triphosphatase (ATPase). Further, X-ray diffraction observations of dried *Tetrahymena* cilia (Silvester, 1964) indicate that the ciliary membrane shares certain diffraction characteristics with nerve myelin.

This study provides new information on the structure of the ciliary membrane obtained with the freeze-etching technique (Steere, 1957; Moor et al., 1961; Moor and Mühlethaler, 1963). This technique has made possible the direct observation of internal membrane structure (Branton, 1969, 1971; Pinto da Silva and Branton, 1970), and, in particular, of small localized membrane differentiations that are thought to be physiologically active regions (Goodenough and Revel, 1970; Chalcroft and Bullivant, 1970; Gilula and Satir, 1971; Gilula et al., 1972). With cilia and flagella, freeze-etching also provides independent confirmation of some axonemal structural details obtained from conventional thin-section electron microscopy. We primarily describe the freeze-etch aspects of cilia of lamellibranch gill epithelium (Fawcett and Porter, 1954; Gibbons, 1961; Satir, 1963), but, in addition, we have sampled motile cilia and flagella from other eukaryotes for comparative purposes. We report, in particular, on a unique differentiation of the ciliary membrane, the *ciliary necklace*. The ciliary necklace, although apparently absent in certain sperm flagellar membranes, is always found in somatic cilia in the transition region where the ciliary membrane joins the plasma membrane and where extensions from the microtubular outer doublets to the ciliary membrane are present. A preliminary report of this work was presented at the 10th Annual Meeting of the American Society for Cell Biology, 1970 (Satir and Gilula, 1970 *b*).

MATERIALS AND METHODS

Freshwater mussels, usually *Elliptio*, were obtained from Carolina Biological Supply Co., Gladstone, Oregon. Gills were excised in the manner described in previous studies (Satir, 1963). Seawater clams, *Mytilus edulis*, were collected at Bodega Marine Laboratory, University of California, Bodega Bay, Calif. The ameboflagellate, *Tetramitus*, was obtained from Dr. W. Balamuth of the Department of Zoology. Sperm of the water fern, *Marsilea vestita*, were obtained from Dr. D. Myles of the Department of Botany. For these studies, embryonic blastulae of the sea urchin, *Strongylocentrotus purpuratus*, were prepared by fertilization and culturing at 15°C. Cultured chick embryo fibroblasts were prepared as previously reported (Pinto da Silva and Gilula, 1972). Common adult male laboratory rats were used to study the tracheal cilia.

For freeze-etching, either small pieces of tissue or cell pellets were fixed briefly (15–20 min) in cacodylate-buffered 3% glutaraldehyde and then placed in cacodylate-buffered 20% glycerol for 1–2 hr before freezing (Branton, 1966). Some pieces of tissue were frozen after distilled water treatment without fixation. All freeze-etching was performed with a Balzers apparatus (Balzers AG, Balzers, Liechtenstein) at −100°C (Moor and Mühlethaler, 1963; Branton, 1966). When no etching was desired, the freeze-fracturing was done at −115°C. The platinum deposition is printed as black and the shadows as white. The shadowing direction is indicated by an arrow on each micrograph.

For thin sections, the tissue was usually fixed in cacodylate-buffered 5% glutaraldehyde (2–4 hr) and postfixed in cacodylate-buffered 1% osmium tetroxide (1 hr). After fixation, the tissue was dehydrated in a graded series of ethanol and then embedded in Epon 812. Thin sections were cut on a Porter-Blum MT-2 or a Huxley ultramicrotome and then stained with uranyl acetate and lead citrate. All observations were made with a Siemens Elmiskop 1A or 101 at 80 kv.

RESULTS

Freeze-Etch of Ciliary Axoneme

NO-ETCH PREPARATIONS: Cross fractures of cilia in preparations without etching generally reveal few axonemal components. The matrix is relatively homogeneous and finely granular. Neither microtubules nor matrix components such as the radial spokes are readily apparent, although there are usually some protrusions present in the region of the nine outer doublets and the central pair (Fig. 1). Occasionally, the 9 + 2 arrangement can be resolved, especially when the ciliary membrane is not present (Fig. 1, inset). Longitudinal fractures of cilia seldom expose components of the axoneme, but usually take a preferential plane through the ciliary membrane.

ETCHED PREPARATIONS: In preparations

that have been etched to remove sublimable material, the homogeneity of the matrix is lost and more information about the axonemal components can be obtained (Fig. 2). The result of etching treatment indicates that the axoneme, except for the well-known structural components, is largely an aqueous solution. In cross fractures of the cilium, the spokes and sometimes the microtubules themselves can be observed. In longitudinal fractures, a period of 1000 A corresponding to the repeat period of the perpendicular spokes is present. The spokes occur as triplets along one microtubule.

In some cases after more extensive etching (1-3 min at −100°C) or possibly melting (since this is only found on the edges of the replicated surface), the convex aspect of the ciliary membrane seems to collapse tightly onto the axonemal contents, producing a "corn-cob" appearance (Fig. 2). The "kernels" responsible for this appearance correspond to the dynein arms resolved with conventional thin sections. The domain of each microtubule is also apparent. Table I compares measurements of the doublet spacing, the dynein periodicity, and the spoke periodicity in sectioned vs. freeze-etched material.

Freeze-Etch of the Ciliary Membrane in the Shaft Region

Upon freeze-fracturing, the ciliary membrane in the shaft region has a convex aspect or fracture face A that is associated with the axonemal side of the membrane, and a concave aspect or fracture face B that is associated with the extracellular side of the membrane (Fig. 1). The convex fracture face (A) contains more membrane-associated particles than the concave fracture face (B). In general the major portion of the ciliary membrane above the transition zone is smooth with few membrane particles that appear to be randomly distributed.

Freeze-Etch of the Ciliary Membrane in the Basal Region

In the neck region of the cilium, just above the juncture of the ciliary membrane with the cell membrane, a dramatic differentiation of the ciliary membrane is revealed with the freeze-etch technique (Figs. 3–8). For obvious reasons, we have termed the most prominent part of this differentiation the "ciliary necklace." Figs. 3 and 4 show fractures through the ciliary necklace of the lateral cilia of the freshwater mussel, *Elliptio*. A comparison of the ciliary necklace region with the adjacent microvilli demonstrates a substantial difference in both the particle content and the particle distribution between the membranes. The microvillar membrane contains many particles—more on its convex than its concave fracture face—without any apparent organized distribution. The ciliary membrane contains fewer particles, but those present are specially organized into strands that comprise the ciliary necklace.

In both *Elliptio* and *Mytilus*, the basal membrane differentiation begins just distal to the basal plate in a region where the membrane is fluted (Fig. 4). On face A, this region often contains a longitudinal arrangement of particles which lie along the flutes and thus correspond to the spacing of the microtubular doublets of the axoneme proper. In *Elliptio*, this arrangement consists of rows of individual particles (Fig. 5), while in *Mytilus* (Fig. 6), the longitudinal array is comprised of small aggregates of particles throughout its length. This unique array does not extend very far apically, but ends abruptly about 0.2–0.45 μm above the basal plate

FIGURE 1 Freeze-fracture of *Elliptio* laterofrontal cilia which reveals the characteristics of the fracture faces in the shaft region and the axoneme without etching. The convex face (*A*) contains more membrane-associated particles than the concave face (*B*). Although there is some indication of peripheral and central structure, the 9 + 2 pattern is not apparent in the cross fractures. Note the ciliary tip (arrow). × 72,000. *Inset:* In the sperm flagella of the fern, *Marsilea*, the ninefold symmetry of the axoneme is more apparent, even without etching. In this case, several axonemes share a single membrane. × 60,000.

FIGURE 2 After extensive etching (or ice sublimation) thin-section components of the ciliary axoneme are more prominent (unfixed specimen). At the lower right, the spokes are seen in a cross-fractured cilium (*). The spokes are also apparent in longitudinal fractures through the axoneme. In some places the triplet arrangement of spokes has been preserved (*t*). The ciliary membranes sometimes have a corn-cob appearance, with the kernels (arrow) having the spacing of the dynein. The domains of individual microtubules extend between the dynein rows. × 45,000.

Published May 1, 1972

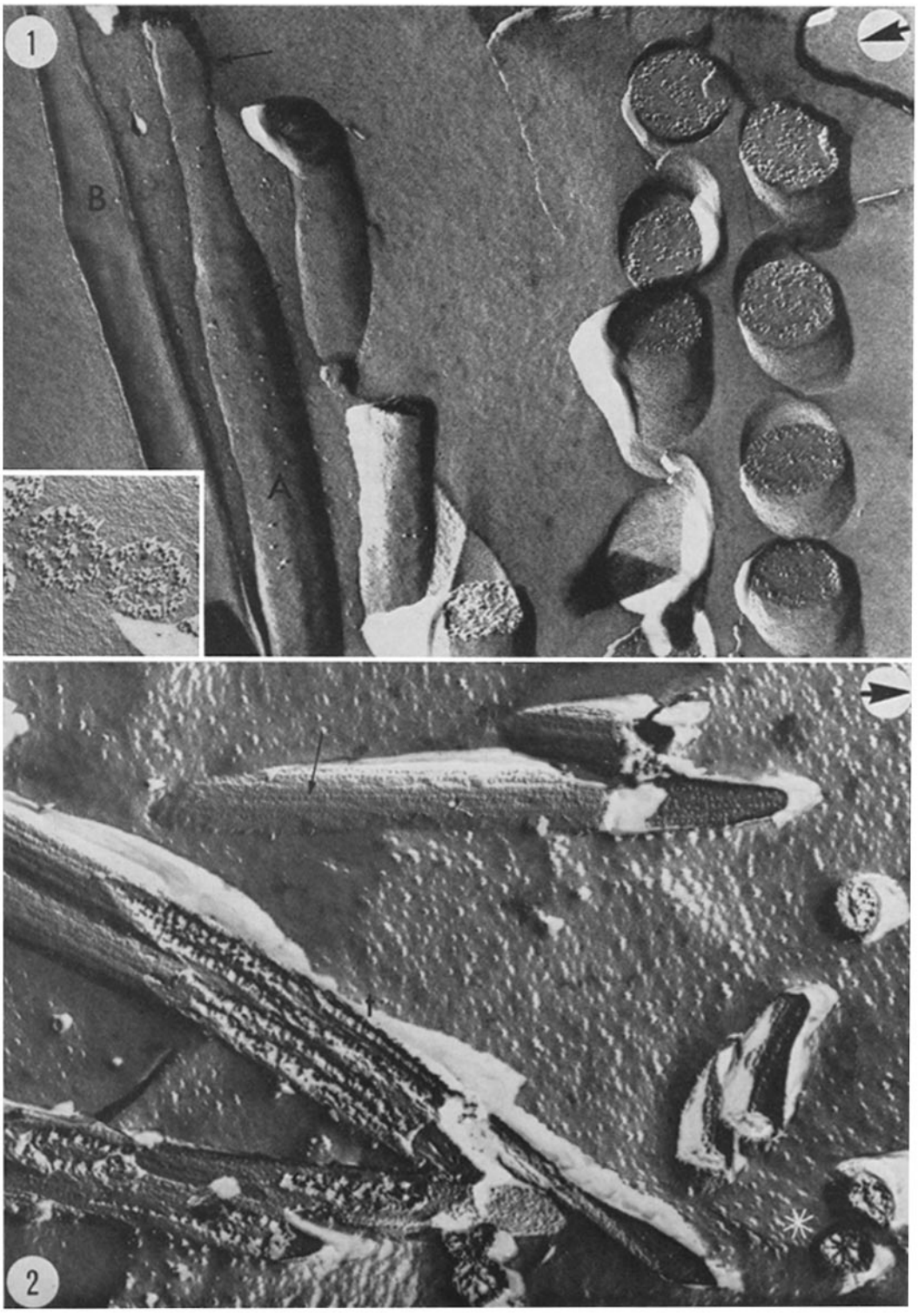

TABLE I

*Structural Measurements of Gill Cilia**

	Sectioned	Freeze-etched
Filament spacing	660	770
Arm periodicity	190	250
Spoke periodicity	960	960
Necklace period	854‡	830
Necklace spacing	460	430
Neck length	1320	900

* Measured in Angstrom units.

‡ Calculated value, based on ciliary diameter.

where the flutes also end. Then at the basal plate the ciliary membrane pinches in. This region is normally devoid of particles, even on fracture face A (Figs. 3, 6–8). Just below this region, the membrane flares out again and the ciliary necklace is visible. All gill cilia examined from lateral, laterofrontal, and frontal cells of any specimen possess identical necklace structures in this region of the ciliary membrane. The necklace is comprised of three strands which are about 450 A apart. The strands consist of scalloped rows containing 90-100-A membrane particles. Measurements indicate that one scallop corresponds to one peripheral doublet (Table I). A direct demonstration of this correspondence is seen in Fig. 6 where the repeating scallops mirror the repeating membrane flutes.

Examination of the necklace region shows that the two membrane fracture faces (A and B) are present (Figs. 3, 4, 6–8). Fracture face A, associated with the axonemal side of the ciliary membrane, contains strands of the ciliary necklace heavily laden with particles. It is continuous with face A of the cell membrane that also contains the particle arrays of the septate and gap junctions (Fig. 3) (Gilula and Satir, 1971). Fracture face B, associated with the extracellular side of the ciliary membrane, possesses fewer particles both within the necklace and in the undifferentiated regions of the membrane. In some views the two fracture faces are clearly complementary; for example, in Fig. 7 scalloped rows of depressions on fracture face B are present at the exact levels that correspond to the scalloped rows of particles on fracture face A of an adjacent cilium. However, in many gill cilia, this complementation is not easy to detect; for, on many B fracture faces, the necklace strands also contain particles (Figs. 4, 8) and, correspondingly, depressions are more difficult to see.

The necklace appears as a standard feature on all somatic cilia that we have studied thus far. At the present time, the necklace has not been seen in the flagellar membranes of either sea urchin or rat sperm (N. B. Gilula, unpublished observations). Among the necklaces that we have studied variations exist in: (*a*) the number of strands that comprise the necklace (Table II), and (*b*) the nature of the strands (scalloped vs. unscalloped). In the freshwater mussel gill, the necklace has three strands (Figs. 3, 4). In the seawater mussel, *Mytilus*, the necklace has three to four strands (Fig. 6). In the ameboflagellate *Tetramitus*, the number of strands is quite variable, and, in some cases, the strands are also incomplete (Fig. 9). In sea urchin blastulae, the number of necklace strands is variable (one to four), and often the strands are incomplete (Fig. 10). The somatic cilium of cultured chick embryo fibroblasts also contains a variable number of incomplete strands (Fig. 11). In the rat trachea, six strands are present (Fig. 12). In all cilia studied thus far, only the molluscan ciliary necklace contains distinctly scalloped strands.

Thin Sections of the Ciliary Necklace Region

In thin sections of cilia, there appears to be a standard cross-sectional appearance of the axoneme (Fig. 14) that corresponds to the necklace region when it is present (Table II). In *Elliptio*, this region lies in the transition zone between the basal plate—that is, the end of the central pair—and the juncture of the ciliary and cell membranes. It is characterized by close packing of the nine doublet microtubules, the lack of the central pair, and a series of specialized connections that extend 50 nm from the midwall of each doublet to the ciliary membrane. The connection is shaped somewhat like a champagne glass, the 15 nm stem joining the microtubules and the 52 nm diameter bowl apposing the membrane. In favorable longitudinal sections (Fig. 13), the three levels of these connections that correspond to the three strands of the ciliary membrane necklace are evident (Fig. 15).

DISCUSSION

Cilia look somewhat different in freeze-etch replicas than in conventional thin sections. In particular, the prominent microtubular 9 + 2 axoneme is not obvious in the replicas. However, under appropriate etching conditions, all of the usual axonemal components—including the 9 + 2 pattern of microtubular doublets—can be detected in their

Published May 1, 1972

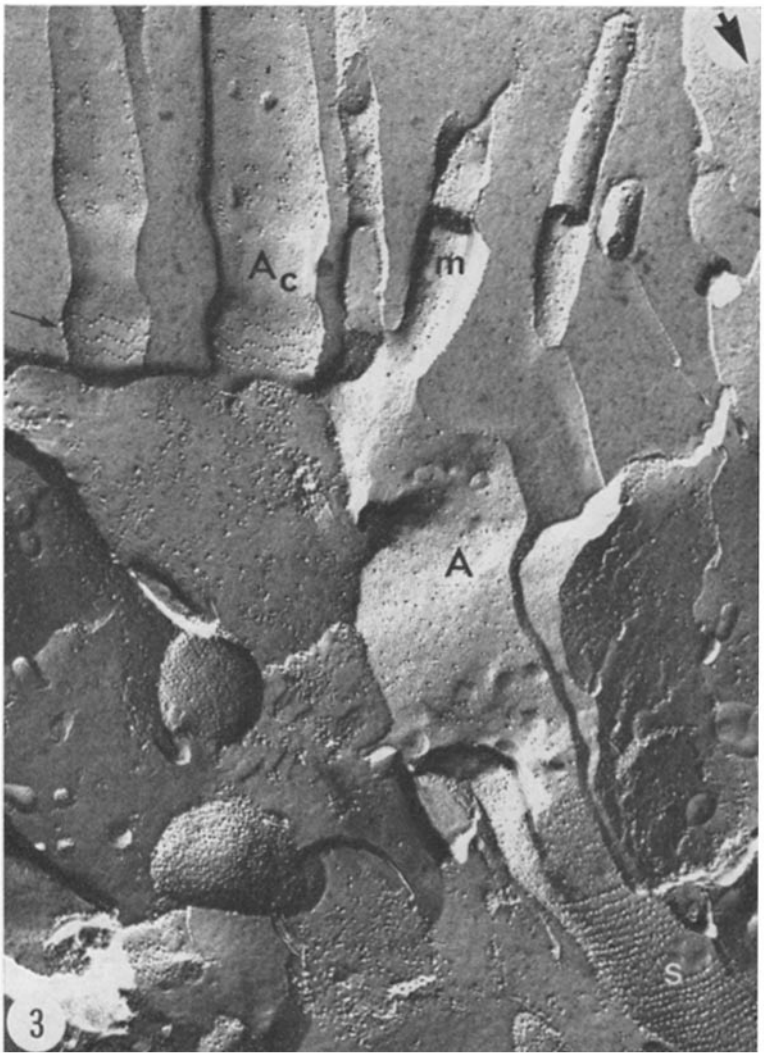

FIGURE 3 Freeze-fracture of apical border of lateral cells from *Elliptio* gill. The A (A_c) faces of the ciliary membranes are present, as well as the A (A) face of the cell membrane. Just above the cell border, the ciliary membranes contain a unique arrangement of three particle strands, the ciliary necklace (arrow), while no necklace is present on the microvilli (m). Note that the face A particles of the ciliary necklace are continuous with the face A of the cell membrane that contains the septate junction (s) particles. × 52,800.

usual relationships to one another. The measurements of axonemal components, including spokes, dynein, and microtubules, are quite comparable to the measurements obtained from thin sections (Table I). Detectable perturbations incurred by the cilium during the freeze-etching process are minimal. Preliminary studies on unfixed isolated outer doublets from sea urchin sperm (N. B. Gilula and J. Bryan, unpublished results) and on intact *Tetrahymena* cilia (Satir et al., 1972) indicate that etching can be used to obtain the subunit structure of microtubules. This information reenforces that obtained with negative-stain or thin-section techniques. Cytoplasmic microtubules which are labile at low temperature can be preserved under the freezing conditions for the freeze-etch technique (Moor, 1967). In a freeze-etch study on the microtubular crystal in a Chrysophycean alga *Pleurochrysis* (Brown and Franke, 1971), even the

Published May 1, 1972

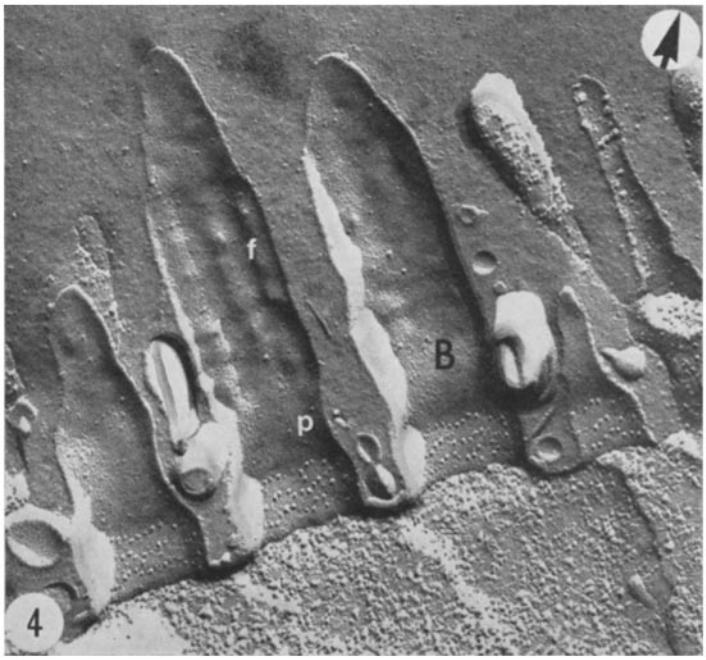

FIGURE 4 Freeze-fracture of the ciliated apical border of *Elliptio* gill lateral cell. The B (*B*) fracture faces of the ciliary membranes are exposed. The B faces contain fewer membrane-associated particles than the A faces (compare with Fig. 3). Above the basal plate (*p*), flutes (*f*) of the ciliary membrane are present. The basal plate region (*p*) is seen on the B face as a bulge that is devoid of particles. Below the basal plate, the B face aspect of the ciliary necklace is present. × 67,500.

bridges between the microtubules are apparent. It can be concluded that even though there may be a great deal of variability in the appearance of microtubules with freeze-etching, this variability seems to be associated with the environment and packing of the microtubules, and not with difficulties of preservation upon freezing. Unfixed specimens can be used for freeze-etching, so that potentially the technique will be useful in testing morphological relationships predicted by models of ciliary motility mechanisms.

There are two major difficulties in observing the longitudinal axonemal contents of cilia with freeze-fracturing. (*a*) The limiting membrane of the cilium provides a preferential fracture plane; consequently, very few longitudinal fractures expose the contents of the cilium. With rat sperm tails, which have a greater diameter than cilia due to their

FIGURES 5 and 6 Fig. 5: *Elliptio* cilia, fracture face A (*A*), showing rows of particles (arrow) in the fluted region above the necklace. Fig. 6: *Mytilus* cilia, fracture face A. In the fluted region, the cilium on the left contains aggregates of particles with the same spacing as the doublets of the axoneme. Note the correspondence of particle rows and necklace scallop periodicity. The cilium on the right contains a large aggregation of particles without a regular organization in the same region of the ciliary membrane. The basal plate region is seen on the A face as a depression (compare with Fig. 4). It is almost devoid of particles. The necklace in *Mytilus* contains three or four strands of particles, and here the last strand is incomplete. Both × 90,000.

FIGURES 7 and 8 Complementary fracture faces in adjacent *Elliptio* cilia. The images in Figs. 7 and 8 were obtained independently, and they do not comprise a complementary pair. The strands of depressions on face B (*B*) are in register with the particle strands of face A (*A*) on the adjacent cilium (lines). The B face strands contain more particles in Fig. 8 than in Fig. 7. Both × 105,000.

Published May 1, 1972

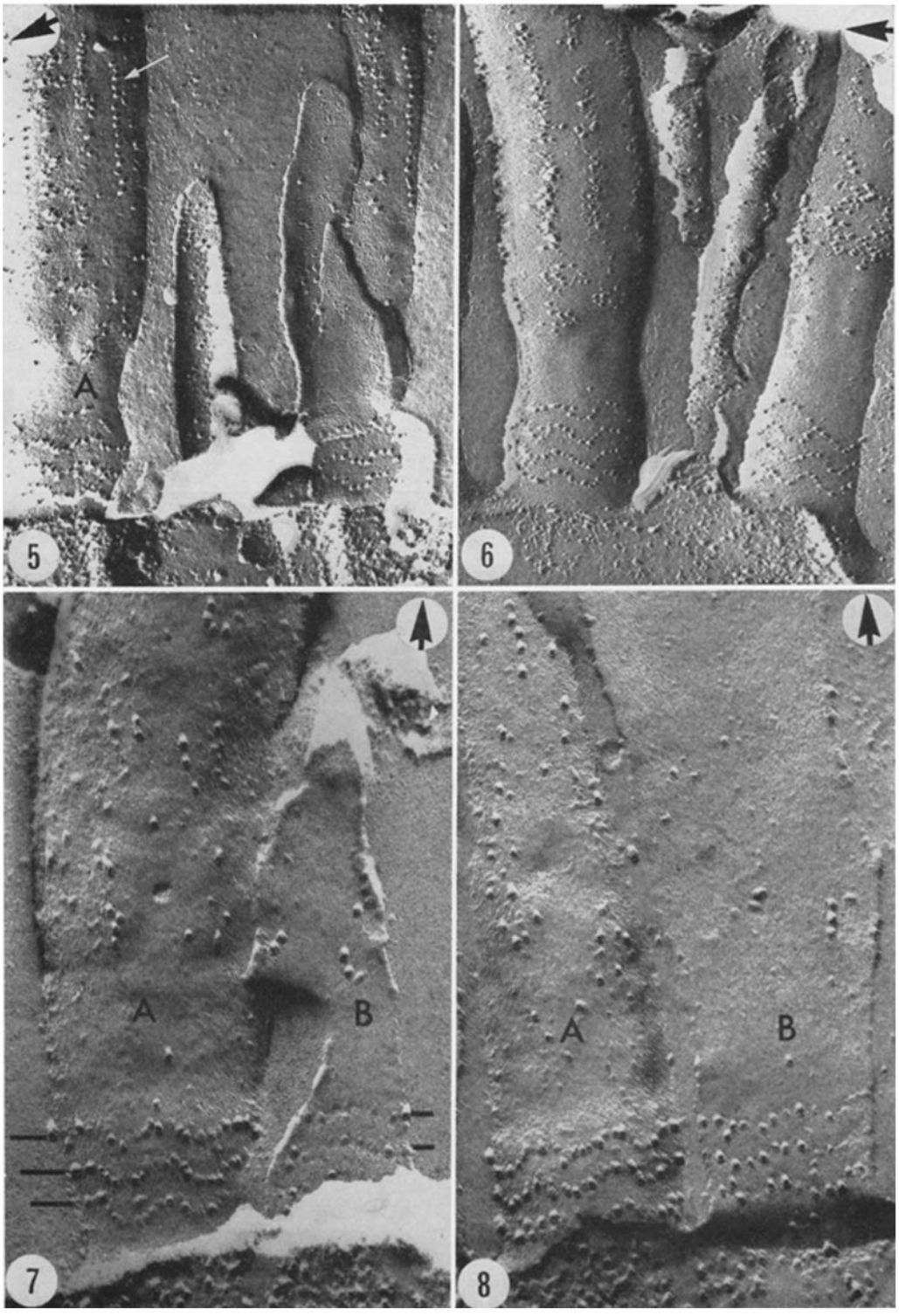

TABLE II

Comparative Aspects of the Ciliary Necklace

Source	Cross-section	Necklace	No. of strands	Reference
Chlamydomonas	+	+	2	G. Ojakian, personal communication
Tetramitus	+	+	3–7	—
Tetrahymena	+	+	2	B. Satir et al., 1972
Sea urchin blastula (*S. purpuratus*)	+	+	1–4	—
Sea urchin sperm (*S. purpuratus*)	−	−	—	N. B. Gilula, unpublished observation
Elliptio gill	+	+	3	—
Mytilus gill	+	+	3–4	—
Fibroblast in culture (Chick embryo)	+	+	1–3	—
Rat trachea	+	+	6	—
Rat sperm	−	−	—	N. B. Gilula, unpublished observation
Mouse oviduct	+	+	6 or more	Dirksen et al., 1971

accessory fibers, the fracture process appears to be more random and the axonemal components can be observed in much greater detail in longitudinal fractures (N. B. Gilula, unpublished results). In fact, individual microtubules, as well as dynein, spoke, and central sheath elements, can easily be observed with little or no etching. (*b*) Due to the small size of the cilium (0.2 μm diameter) and its high water content, the axoneme appears relatively homogeneous (with a few protrusions) after freezing. The limiting spaces seen around the axonemal components in thin sections are not visible after freeze-fracture because they are actually filled with ice and usually there is no difference in height to provide contrast. Similarly, this seems to be true for the material within the microtubule. Presumably, this material is unstained in thin sections because of its limited organic content. With extensive etching after distilled water pretreatment of unfixed specimens, the microtubules become visible. Material both in the matrix and in the center of the microtubule is sublimable during the etching process. These regions presumably contain ice or sublimable materials.

The original hypothesis of Branton (Branton, 1966) proposed that, in freeze-etching, membranes fracture internally along a unique plane to produce two fracture faces that are complementary. Recent labeling experiments (Pinto da Silva and Branton, 1970; Tillack and Marchesi, 1970) have produced affirmative evidence that the true surfaces of membranes are not exposed by the freeze-etch process. Also, double replica techniques have shown that membranes do possess a single fracture plane (Chalcroft and Bullivant, 1970; Wehrli et al., 1970). The evidence therefore suggests that the freeze-fracture process exposes internal components (fracture faces) of cell membranes that lie on a unique fracture plane within the membrane. In some cases, the continuous aparticulate background of the fractured membrane probably corresponds to the middle of a lipid bilayer (Deamer and Branton, 1967; Branton, 1967). The particles represent a deviation in the normal fracture plane. Additional information suggests that the membrane particles are, in part, determined by protein components of the membrane (Branton, 1971; Pinto da Silva et al., 1971); and, more recently, that the particles (Pinto da Silva et al., 1971) as well as certain membrane proteins (Bretscher, 1971; Steck et al., 1971) may traverse the thickness of the membrane. Therefore, the appearance of a particle on fracture face A or B may be a consequence of a differential bonding of the particle at either side of the membrane. The ratio of numbers of similar particles on the two fracture faces may be analogous to a bonding partition coefficient.

In the case of the ciliary membrane two distinct membrane appearances are produced by the fracture process: (*a*) a convex component (A) with few random particles; and (*b*) a concave component (B) with even less particles. The relative absence of particles may be taken to suggest the relative absence of protein intercalations in the ciliary

Published May 1, 1972

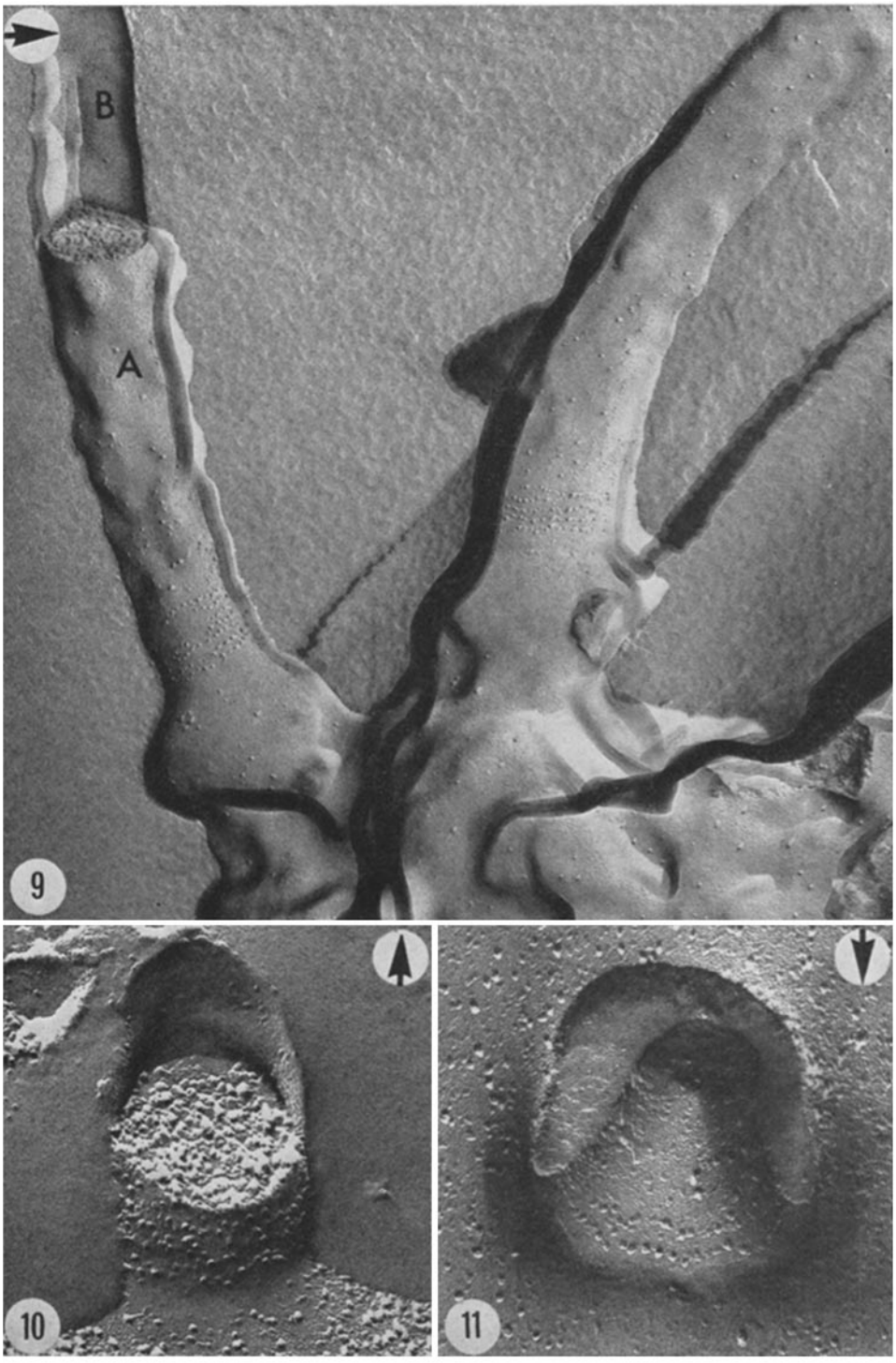

FIGURE 9 Freeze-fracture of two flagella of the ameboflagellate *Tetramitus*. Few particles are present in the shaft region on either face A (*A*) or B (*B*). The necklace region contains a variable number of unscalloped particle strands. × 70,000.

FIGURE 10 Freeze-fracture revealing the ciliary necklace of a cilium from the sea urchin blastula. × 120,000.

FIGURE 11 The ciliary necklace from a somatic cilium of cultured chick embryo fibroblast. × 84,000.

Published May 1, 1972

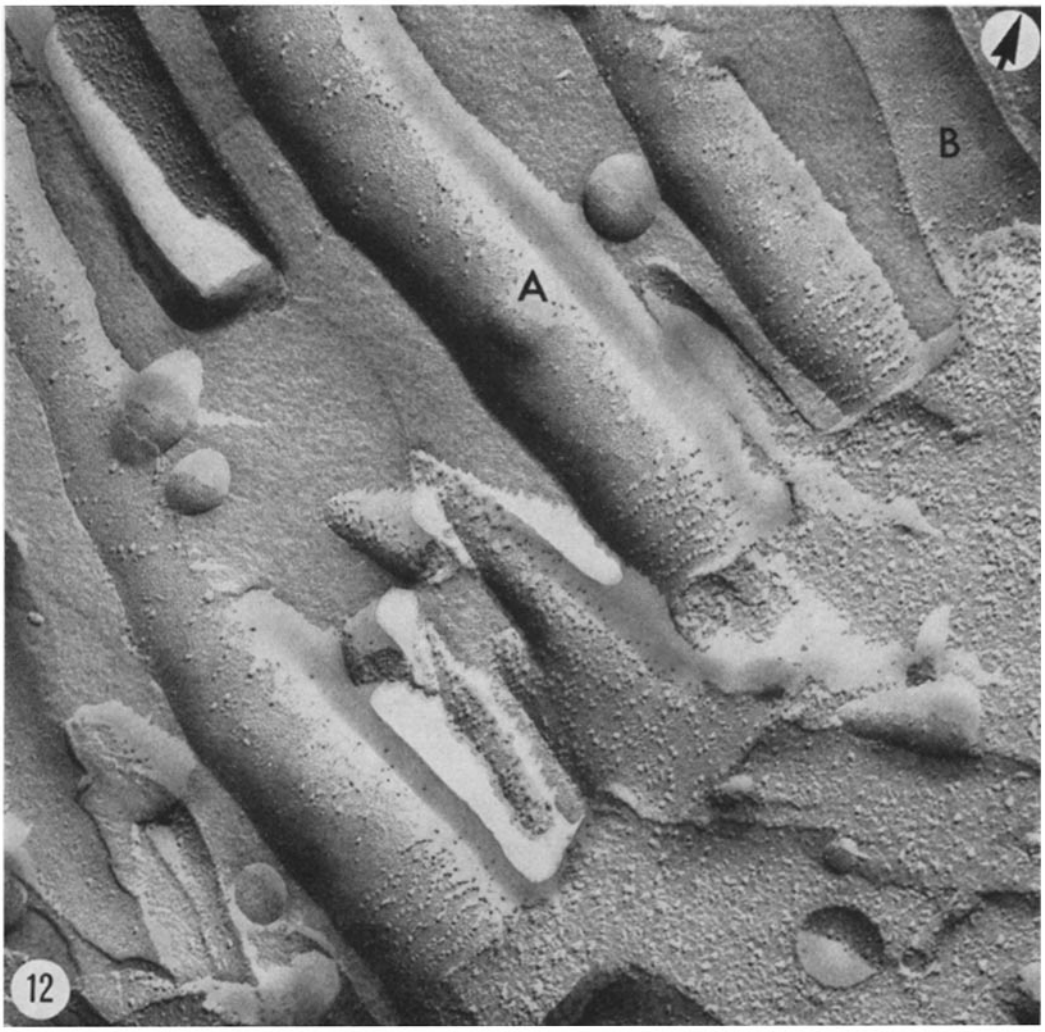

FIGURE 12 Fracture faces (*A* and *B*) of cilia from rat tracheal epithelium. These cilia contain six particle strands in their necklace region. × 80,000.

membrane, and perhaps indicates that the ciliary membrane is comprised largely of a lipid bilayer. At the basal end of the cilium where thin sections reveal a special series of relationships between microtubules and membrane, freeze-etching reveals corresponding particle arrangements on face A. The flutes on the membrane are easily visualized by this technique and face A sometimes contains lines of particles corresponding to the microtubules. This particle arrangement also has been seen in insect sperm flagellar membranes (Baccetti et al., 1971). Just at the basal plate where the membrane pinches in close to the axoneme, freeze-etch particles are conspicuously and consistently absent.

The most striking structural feature of the cilium that is revealed by freeze-etching is undoubtedly the ciliary necklace. This unique membrane differentiation even matches certain cell junctions (Goodenough and Revel, 1970; Chalcroft and Bullivant, 1970; Gilula et al., 1970; Gilula and Satir, 1971) in terms of its complexity and restricted nature. In the ciliary necklace region, fracture face A contains complete strands of particles and is continuous with fracture face A of the cell membrane; fracture face B, on the other hand,

Published May 1, 1972

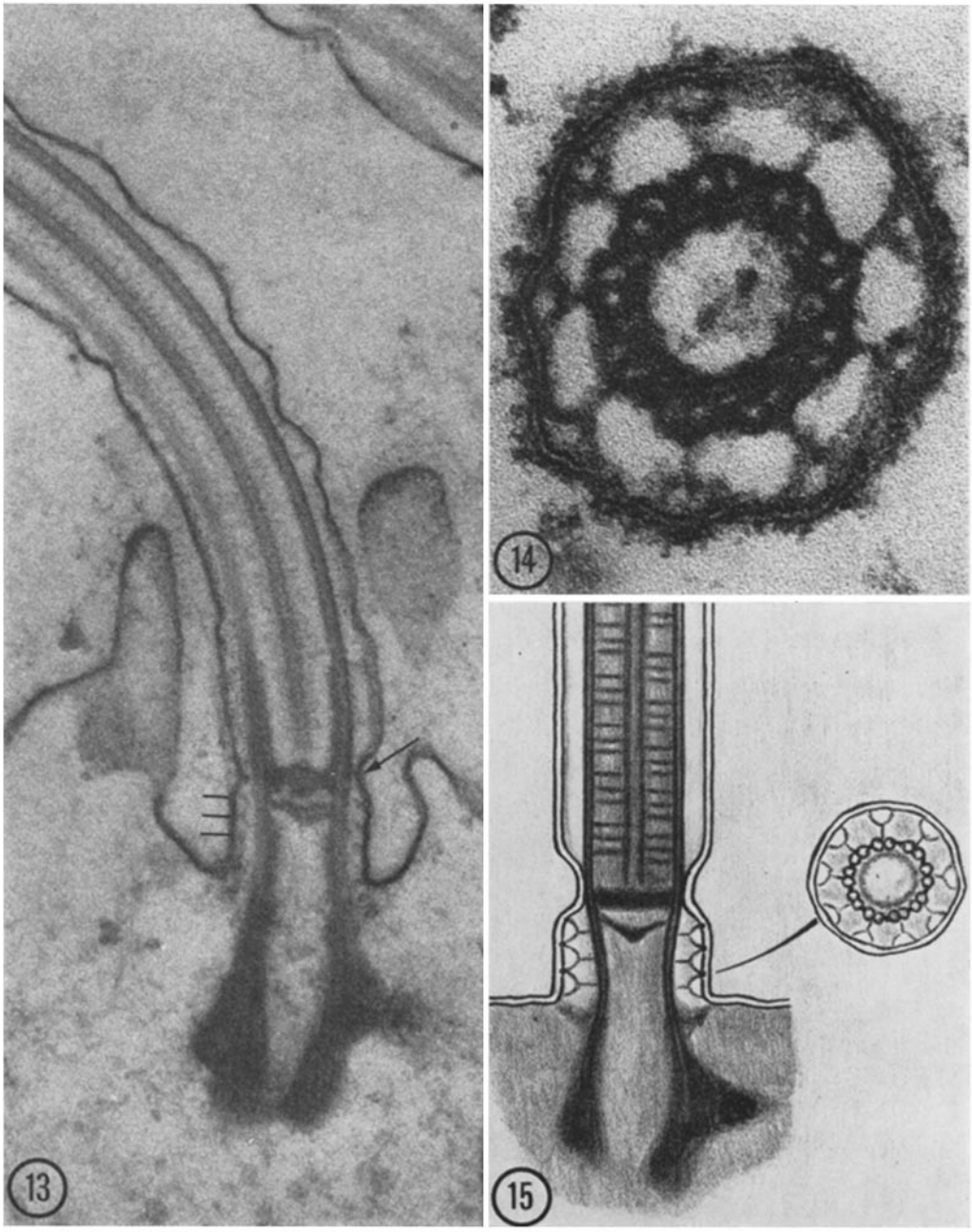

FIGURE 13 Thin section through longitudinal plane of an *Elliptio* lateral cilium which contains a longitudinal view of the thin-section necklace components. The membrane pinches in at the basal plate (arrow). Below the basal plate, the necklace region contains three bowls or cups (lines) which are apposed against the membrane. × 80,000.

FIGURE 14 Cross-section of *Elliptio* cilium through the necklace region. From the midwalls of the microtubular doublets, the "champagne glasses" extend to the ciliary membrane. The glasses are comprised of a short segment or stem which extends from the doublet midwall to the bowl or cup of the glass. The cup, in turn, extends to the membrane, thus producing a membrane-microtubule complex × 240,000.

FIGURE 15 Schematic representation of the thin-section longitudinal and cross-section information of the ciliary necklace region in *Elliptio.*

Published May 1, 1972

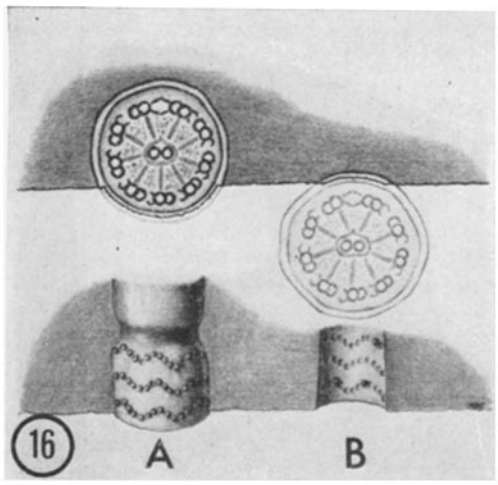

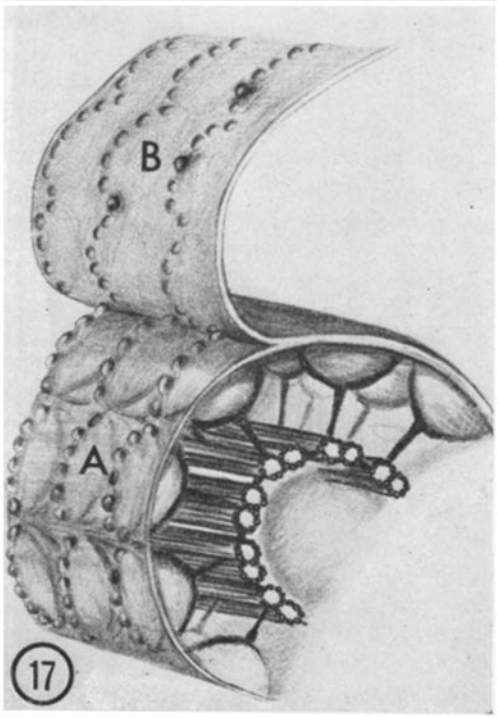

FIGURE 16 Schematic interpretation of the fracture process of the ciliary membrane necessary to produce the fracture faces of Figs. 7 and 8. The convex fracture face (*A*) is obtained when a portion of the membrane is torn away during the fracture process. Face A apposes the axoneme. The concave fracture face (*B*) apposes the exterior; the entire axoneme and a portion of the membrane is torn away during the fracture process.

FIGURE 17 Three-dimensional interpretation of the membrane-microtubule complex of the ciliary necklace. The champagne glass extensions seen in Fig. 10 connect the intramembrane particles (exposed with freeze-fracture) and the microtubular doublets of the axoneme.

contains fewer particles per strand, and, in some cases, strands of depressions in alignment with the particle-containing strands of face A (Fig. 7). We interpret these as complementary fracture faces as shown in Figs. 16 and 17. Complementation between A and B faces in the necklace region is not always apparent in gill cilia. In the future, information from the double replica procedure (Chalcroft and Bullivant, 1970; Wehrli et al., 1970) should be useful for further understanding the particle alignment between the two fracture faces in the ciliary necklace region.

Recently, Flower (1971) has demonstrated that the membrane particles of the molluscan ciliary necklace reside within the ciliary membrane and that they can be visualized as protuberances on the membrane surface exposed by extensive etching. After extensive etching, however, the membrane often shrinks down around the axoneme or axonemal extensions and outlines them (as in Fig. 2). In the absence of additional information on the membrane surface in the necklace region in unetched preparations, we have chosen to represent the surface as smooth (Fig. 17).

Our interpretation of the correspondence of the ciliary necklace with the thin section information for mussel gill cilia is schematically represented in Fig. 17. The precise correspondence of the membrane particles with the cuplike extensions is not known. Two relationships seem possible: either (*a*) the particles lie in the center of the cups; or (*b*) alternatively, as is represented in the diagram, the particles lie along one edge of the cuplike extensions from the microtubules. The placement of the particles at the edge of the cups would account for the scalloping of the rows. Either arrangement essentially produces the same result; the correspondence of the necklace particles to the cuplike extensions which provides a possible structural link from the doublet midwall to the exterior. In essence, a potential functional "membrane-microtubule complex" is present.

There are several potential functions for the ciliary necklace and also the membrane-microtubule complex. Most studies of motile eukaryotic cilia have primarily dealt with the mechanism of motility. It has been demonstrated that cilia and sperm flagella may be reactivated under conditions (glycerination, detergent treatment) where the limiting membrane has been disrupted or lost (Brokaw, 1961; Satir, 1965; Gibbons, 1965; Gibbons and Gibbons, 1969). In these studies it is clear that beating of these organelles may occur without an intact limiting membrane, and that the

ciliary membrane can only be required as a barrier to the random diffusion of ATP and cations. Therefore, the ciliary necklace probably does not have a significant role in the actual mechanism of motility or beating. The necklace may, instead, turn out to be involved in the control of localized membrane permeability, that is, this region may prove to be an energy tranducing zone of the cilium, perhaps part of the timer of ciliary beat. A relationship between direction of the effective stroke and membrane potential already has been established for some cilia (Kinosita, 1954). This probably is mediated in part by an influx of Ca^{++} through specific regions in the membrane (Eckert and Naitoh, 1970). It is possible that the necklace particles are membrane mechanoenzymes or that they serve as ionic permeability sites. Changing ion flux might provide a feedback control for turning on or off microtubule sliding. This mechanism might also operate in reverse, that is, for mechanosensitivity of motile cilia and mechanoreception in ciliary receptors. The necklace is arranged so that microtubule sliding, whether part of the continuous ciliary stroke or mechanically induced in a rigid nonmoving cilium, will cause specific alterations in the particle patterns.

An examination of the comparative distribution of the ciliary necklace and its corresponding cross-section provides additional clues as to its possible functional significance. For example, with the exception of sperm flagella, the ciliary necklace appears to be as universally associated with motile somatic cilia and flagella as is the ninefold symmetry of the axonemal doublets. So far, sperm do not appear to possess the necklace; in fact, the entire membrane-microtubule complex described above is absent. The absence of the ciliary necklace in sperm flagella may actually reflect an important difference in their control mechanism. Sperm flagella are normally "turned-on" in an irreversible manner, which is not normally affected until their short life-span is completed. However, somatic cilia and flagella have a much longer life-span and, in most cases, particularly in unicellular organisms, they may serve multiple functions and must be capable of responding to a variety of environmental stimuli.

Although there is not yet any freeze-etch information available on sensory (modified) cilia, with the exception of the 9 + 0 cilium from a fibroblast in culture (Fig. 11), it is interesting to note that the typical cross-section corresponding to the necklace region is present in the vertebrate ear and in certain insect mechanoreceptors such as the campaniform sensillum. The examination of isolated cilia removed for biochemical studies reveals that the necklace region of the ciliary membrane remains attached to the cell.

The ciliary necklace also can be used as a morphological marker for the study of generation of the ciliary membrane. Reports suggest that during the genesis of a cilium, new components are continually assembled at the apical region of the generating organelle (Rosenbaum et al., 1969). Preliminary studies on *Tetrahymena* cilia (Satir et al., 1972) and on mouse oviduct cilia (Davidson et al., personal communication) suggest that the ciliary necklace is the initial membrane differentiation produced during the assembly of a new cilium. It may be that some of the variability seen in the numbers of necklace strands in oviduct cilia, *Tetramitus* flagella, and sea urchin blastula cilia is morphogenetic. Since the necklace is formed initially, all new membrane components must be intercalated around the necklace particles or added above the necklace region.

We thank Dr. Daniel Branton for use of the freeze-etch facilities, and also Michael Gurfinkiel for photographic assistance. We also appreciate the staff assistance and use of the facilities of the Scientific Photography and Electron Microscope Laboratories.

This work was supported by grants from the United States Public Health Service (HE 13849) to Dr. Satir, and AEC AT (04-3)-34 P.A. 142 to Dr. Branton. Dr. Gilula was a United States Public Health Service predoctoral trainee under grant GM 1021.

Received for publication 22 November 1971, and in revised form 19 January 1972.

REFERENCES

AFZELIUS, B. 1959. Electron microscopy of the sperm tail; results obtained with a new fixative. *J. Biophys. Biochem. Cytol.* **5**:269.

BACCETTI, B., E. BIGLIARDI, and F. ROSATI. 1971. The spermatozoon of Arthropoda. XIII. The cell surface. *J. Ultrastruct. Res.* **35**:582.

BRANTON, D. 1966. Fracture faces of frozen membranes. *Proc. Nat. Acad. Sci. U. S. A.* **55**:1048.

BRANTON, D. 1967. Fracture faces of frozen myelin. *Exp. Cell Res.* **45**:703.

BRANTON, D. 1969. Membrane structure. *Annu. Rev. Plant Physiol.* **20**:209.

BRANTON, D. 1971. Freeze-etching studies of mem-

brane structure. *Phil. Trans. Roy. Soc. London Ser. B Biol. Sci.* **261**:133.

BRETSCHER, M. S. 1971. A major protein which spans the human erythrocyte membrane. *J. Mol. Biol.* **59**:351.

BROKAW, C. J. 1961. Movement and nucleoside polyphosphatase activity of isolated flagella from *Polytoma uvella*. *Exp. Cell. Res.* **22**:151.

BROWN, R. M., and W. W. FRANKE. 1971. A microtubular crystal associated with the Golgi field of *Pleurochrysis scherffelii*. *Planta.* **96**:354.

CHALCROFT, J. P., and S. BULLIVANT. 1970. An interpretation of liver cell membrane and junction structure based on observation of freeze-fracture replicas of both sides of the fracture. *J. Cell Biol.* **47**:49.

DEAMER, D. W., and D. BRANTON. 1967. Fracture planes in an ice bilayer model membrane system. *Science (Washington).* **158**:655.

DIRKSEN, E. R., N. B. GILULA, L. DAVIDSON, C. SCHOOLEY, B. SATIR, and P. SATIR. 1971. New aspects of cilia structure. *Anat. Rec.* **169**:464.

ECKERT, R., and Y. NAITOH. 1970. Passive electrical properties of *Paramecium* and problems of ciliary coordination. *J. Gen. Physiol.* **55**:467.

FAWCETT, D. W., and K. R. PORTER. 1954. A study of the fine structure of ciliated epithelia. *J. Morphol.* **94**:221.

FLOWER, N. E. 1971. Particles within membranes: a freeze-etch view. *J. Cell Sci.* **9**:435.

GIBBONS, B. H., and I. R. GIBBONS. 1969. Reactivation of sea urchin sperm after extraction with Triton X-100. *J. Cell Biol.* **43**(2, Pt. 2):43 a. (Abstr.)

GIBBONS, I. R. 1961. The relationship between fine structure and beat in the gill cilia of a lamellibranch mollusc. *J. Biophys. Biochem. Cytol.* **11**:179.

GIBBONS, I. R. 1963. Studies on the protein components of cilia from *Tetrahymena pyriformis*. *Proc. Nat. Acad. Sci. U. S. A.* **50**:1002.

GIBBONS, I. R. 1965. Reactivation of glycerinated cilia from *Tetrahymena pyriformis*. *J. Cell Biol.* **25**:400.

GIBBONS, I. R. 1967. The structure and composition of cilia. *In* Symposium of the International Society for Cell Biology. K. Warren, editor. Academic Press Inc., New York. **6**:99.

GIBBONS, I. R., and A. V. GRIMSTONE. 1960. On flagellar structure in certain flagellates. *J. Biophys. Biochem. Cytol.* **7**:697.

GILULA, N. B., D. BRANTON, and P. SATIR. 1970. The septate junction: a structural basis for intercellular coupling. *Proc. Nat. Acad. Sci. U. S. A.* **67**:213.

GILULA, N. B., O. R. REEVES, and A. STEINBACH. 1972. Metabolic coupling, ionic coupling, and cell contacts. *Nature (London).* **235**:262.

GILULA, N. B., and P. SATIR. 1971. Septate and gap junctions in molluscan gill epithelium. *J. Cell Biol.* **51**:869.

GOODENOUGH, D. A., and J. P. REVEL. 1970. A fine structural analysis of intercellular junctions in the mouse liver. *J. Cell Biol.* **45**:272.

KINOSITA, H. 1954. Electrical potentials and ciliary response in *Opalina*. *J. Fac. Sci. Univ. Tokyo. Sect. I.* **7**:1.

MANTON, I., and B. CLARK. 1952. An electron microscope study of the spermatozoid of *Sphagum*. *J. Exp. Bot.* **3**:265.

MOOR, H. 1967. Der Feinbau der Mikrotubuli in Hefe nach Gefrieratzung. *Protoplasma.* **64**:89.

MOOR, H., and K. MÜHLETHALER. 1963. Fine structure in frozen-etched yeast cells. *J. Cell Biol.* **17**: 609.

MOOR, H., K. MÜHLETHALER, H. WALDNER, and A. FREY-WYSSLING. 1961. A new freezing ultramicrotome. *J. Biophys. Biochem. Cytol.* **10**:1.

PINTO DA SILVA, P., and D. BRANTON. 1970. Membrane splitting in freeze-etching. *J. Cell Biol.* **45**: 598.

PINTO DA SILVA, P., S. D. DOUGLAS, and D. BRANTON. 1971. Localization of A antigen sites on human erythrocyte ghosts. *Nature (London).* **232**:194.

PINTO DA SILVA, P., and N. B. GILULA. 1972. Gap junctions in normal and transformed fibroblasts in culture. *Exp. Cell Res.* In press.

PORTER, K. R. 1957. The submicroscopic morphology of protoplasm. *Harvey Lect.* **51**:175.

RONKIN, R. R., and K. M. BURETZ. 1960. Sodium and potassium in normal and paralyzed *Chlamydomonas*. *J. Protozool.* **7**:109.

ROSENBAUM, J. L., J. E. MOULDER, and D. L. RINGO. 1969. Flagellar elongation and shortening in *Chlamydomonas*. *J. Cell Biol.* **41**:600.

SATIR, B., C. SCHOOLEY, and P. SATIR. 1972. The ciliary necklace in *Tetrahymena*. In Symposium on Motile Cell Systems. *Acta Protozool.* In press.

SATIR, P. 1963. Studies on cilia. The fixation of the metachronal wave. *J. Cell Biol.* **18**:345.

SATIR, P. 1965. Structure and function in cilia and flagella. *Protoplasmatologia.* III E.

SATIR, P., and N. B. GILULA. 1970 *a*. The cell junction in a lamellibranch gill ciliated epithelium. *J. Cell Biol.* **47**:468.

SATIR, P., and N. B. GILULA. 1970 *b*. Freeze-etch of cilia. *J. Cell Biol.* **47**(2, Pt. 2):179 a. (Abstr.)

SILVESTER, N. R. 1964. The cilia of *Tetrahymena pyriformis*: X-ray diffraction by the ciliary membrane. *J. Mol. Biol.* **8**:11.

STECK, T. L., G. FAIRBANKS, and D. F. H. WALLACH. 1971. Disposition of the major proteins in the isolated erythrocyte membrane. Proteolytic dissection. *Biochemistry.* **10**:2617.

STEERE, R. L. 1957. Electron microscopy of structural

detail in frozen biological specimens. *J. Biophys. Biochem. Cytol.* **3**:45.

STEINBACH, H. B., and P. B. DUNHAM. 1962. Ionic balance in sperm cells. *In* Spermatozoan Motility. D. W. Bishop, editor. American Association for the Advancement of Science, Washington, D.C. 55.

TILLACK, T. W., and V. T. MARCHESI. 1970. Demonstration of the outer surface of freeze-etched red blood cell membranes. *J. Cell Biol.* **45**:649.

WEHRLI, E., K. MÜHLETHALER, and H. MOOR. 1970. Membrane structure as seen with a double replica method for freeze-fracturing. *Exp. Cell Res.* **59**:336.